

Document downloaded from:

<http://hdl.handle.net/10251/38718>

This paper must be cited as:

Laurí Pla, D.; Sanchís Saez, J.; Martínez Iranzo, MA. (2013). Latent variable based model predictive control: Ensuring validity of predictions. *Journal of Process Control*. 23(1):12-22. doi:10.1016/j.jprocont.2012.11.001.



The final publication is available at

<http://dx.doi.org/10.1016/j.jprocont.2012.11.001>

Copyright International Federation of Automatic Control (IFAC)

Latent Variable based Model Predictive Control: Ensuring Validity of Predictions

D. Laurí^{a,*}, J. Sanchis^a, M. Martínez^a, A. Hilario^a

^a *Instituto Universitario de Automática e Informática Industrial
Universidad Politécnica de Valencia
Camino de Vera s/n, Valencia 46022, Spain*

Abstract

This paper presents a methodology to constrain the optimization problem in LV-MPC so that validity of predictions can be ascertained. LV-MPC is a model-based predictive control methodology implemented in the space of the latent variables and is based on a linear predictor. Provided real processes are non-linear, there is model-process mismatch, and under tight control, the predictor can be used for extrapolation. Extrapolation leads to bad predictions which deteriorates control performance, hence the interest in validity of predictions. In the proposed approach first two validity indicators on predictions are defined. The novelty in the two indicators proposed is they neglect past data, and so validity of predictions is ascertained in terms of future moves which are actually the degrees of freedom in the optimization. Second, the indicators are introduced in the optimization as constraints. Provided the indicators are quadratic, recursive optimization with linearised constraints is implemented. A MIMO example shows how ensuring validity of predictions neglecting past data can improve closed-loop performance, specially under tight control outside the identification region.

Key words: Data-driven, Model Predictive Control, Latent Variable, Prediction, Control Relevant Identification, Validity of predictions

1. Introduction

In large-scale manufacturing processes such as chemical, food, or steel making processes; there are a large number of CVs (Controlled Variables), and MVs (Manipulated Variables). Due to the multivariate nature of the data, variables are highly correlated, and the effective dimension of the space in which they move is very small. LVMs (Latent Variable Methods) can transform noisy and correlated data into a smaller informative

*Corresponding author. Tel.: +34 963879770; Fax: +34 963879579.

Email addresses: dalau1@upv.es (D. Laurí)

Preprint submitted to Journal of Process Control

October 28, 2012

set defined by the latent variables [1]. Another tool widely used in the process industry is Model-based Predictive Control (MPC). MPC is widely used in industry due to its ability to handle multivariable systems subject to input and output constraints [2, 3, 4].

The combination of these two powerful tools yields LV-MPC. LV-MPC is a model-based predictive control methodology implemented in the space of the latent variables. LV-MPC can be applied to batch [5] and continuous [6] processes. The advantages of using LV-MPC include:

- In LV-MPC, the dynamic matrices used to perform multi-step ahead predictions are obtained directly from process data [7, 8]. Therefore, the model obtained is commensurate with its final use. This is often denoted MPC Relevant Identification (MRI).
- Provided latent variable techniques are used for model identification, data requirements for the identification data set are very modest.
- MPC optimization is performed in the space of the latent variables. Then problems with large control horizon can be solved at a reasonable computational cost. Alternatives to this approach in MPC include move blocking strategies [9] and the use of Laguerre functions [10].
- Latent variable methods provide indicators of validity of the model referred to the identification data set. Such indicators can be used in the optimization in LV-MPC to constrain the decision space and avoid using the model for extrapolation. Consequently, better predictions can be obtained, specially under tight control and in the event of disturbances or faults. Finally, better predictions lead to better closed loop performance in MPC.

The second point in the list is normally the main reason that motivates using PLS as it can deal with correlation in the data set. However, this paper focuses on the last item on the list: Ensure Validity of Predictions in LV-MPC. Although industrial processes are non-linear, most implemented control solutions are based on linear models [11, 12]. LV-MPC is based on a linear structure for predictions, thus there is model-process mismatch. Under tight control, the predictor may be used in extrapolation mode leading to erratic control moves. In [13] Hotelling's T^2 index is weighted in the MPC cost function to avoid decisions using the model outside its validity range. In [6] Hotelling's T^2 index along with squared residuals in the input space are weighted in the MPC cost function. Weighting such indices in the MPC cost function can avoid the optimization to use the model outside its validity range, but yields the following drawbacks:

- (I) If past data is in a region outside the region spanned by the identification data set, validity indicators provide a large value regardless of the future trajectory of the MVs. This alters the MPC cost function not necessarily helping to decide a better future trajectory for the MVs.

- (II) The weights are additional parameters that need be tuned. Small weights allow using the model in extrapolation, and large weights alter the resulting decision of the controller. There is no tuning strategy to ascertain validity of predictions in any situation.

The approach to ensure validity of predictions proposed in this paper overcomes the two drawbacks commented above.

- (I) Two validity indicators based on Hotelling's T^2 and the squared residuals in the input space are defined. The novelty in the indicators defined is they neglect past data.

If validity indicators are considered in LV-MPC, the decision of the controller tries to keep validity indicators inside the valid range. If validity indicators contain past data, and past data lays outside the region spanned by the identification data set, validity indicators provide large values regardless of the future trajectory of the MVs. Consequently, there may be no solution of the MVs to keep validity indicators in the valid region because it is the past what causes the indicators to present large values. If past data is neglected however, validity indicators define which future trajectories are acceptable compared to those used for identification. Consequently, the decision of the controller is not constrained by the past, which cannot be changed, but by having acceptable future trajectories of the manipulated variables so that the predictor is not used in extrapolation.

- (II) Validity indicators are added as constraints in LV-MPC. Such indicators are quadratic in the variable of decision, then the resulting problem is a QCQP (Quadratically Constrained Quadratic Program). The QCQP is solved as a sequence of QPs (Quadratic Programs) with linearisation of quadratic constraints. To reduce the number of QPs that need be solved at each sampling time, linearisation of each quadratic constraint is performed at the boundary of the constraint aligned with the current point and the minimum of the constraint. Adding constraints instead of weighting the validity indices in the cost function forces the decision to ascertain validity of the model whilst the LV-MPC cost function remains unaltered. The drawback in this approach is the increase in computational complexity to solve a sequence of QPs.

The structure of this paper is as follows: The LV-MPC approach for continuous processes in [6] is summed up in Section 2. The validity indicators proposed in this paper are introduced in Section 3. How to include the validity indicators in LV-MPC as constraints is explained in Section 4. In Section 5, a MIMO example shows how ensuring validity of predictions can improve closed-loop performance, specially under tight control and in the event of working outside the identification region. The paper ends with concluding remarks in Section 6.

2. LV-MPC methodology

LV-MPC for continuous processes is presented in [6]. This Section briefly describes the LV-MPC methodology and reformulates the most relevant formulas in the sake of readability of the present paper. For further details, the reader is referred to [6].

2.1. Model structure

The following linear structure for predictions is used in LV-MPC:

$$\hat{\mathbf{y}}_f(k) = \overbrace{\left[\underbrace{\mathbf{u}_p(k)}_{\triangleq \mathbf{x}_p(k)} \quad \underbrace{\mathbf{y}_p(k)}_{\triangleq \mathbf{x}_f(k)} \quad \underbrace{\mathbf{u}_f(k)}_{\triangleq \mathbf{x}_{\text{dof}}(k)} \quad \underbrace{\mathbf{u}_{\text{dof}}(k)}_{\triangleq \mathbf{x}_{\text{dof}}(k)} \right]}^{\mathbf{x}(k)} \boldsymbol{\theta} \quad (1)$$

where $\boldsymbol{\theta}$ is the dynamic matrix with appropriate dimensions, and

$$\hat{\mathbf{y}}_f(k) = [\mathbf{y}_{k+1} \ \dots \ \mathbf{y}_{k+n_f}] \quad (2)$$

$$\mathbf{u}_p(k) = [\mathbf{u}_{k-1} \ \mathbf{u}_{k-n_b+1}] \quad (3)$$

$$\mathbf{y}_p(k) = [\mathbf{y}_{k-1} \ \mathbf{y}_{k-n_a}] \quad (4)$$

$$\mathbf{u}_f(k) = [\mathbf{u}_{k+n_f-1} \ \dots \ \mathbf{u}_{k+n_u}] \quad (5)$$

$$\mathbf{u}_{\text{dof}}(k) = [\mathbf{u}_{k+n_u-1} \ \dots \ \mathbf{u}_k] \quad (6)$$

where: n_f , prediction horizon; n_b , past horizon for inputs; n_a , past horizon for outputs; n_u , control horizon; $\mathbf{y}_k \in \mathbb{R}^{1 \times n_o}$; n_o , number of outputs; $\mathbf{u}_k \in \mathbb{R}^{1 \times n_i}$; and n_i , number of inputs.

2.2. Identification in the latent variable space

Identification data matrices can be obtained from Equation (1) for $k \in [1 \dots N]$, and PLS is used for identification [14].

$$\mathbf{X} = \mathbf{T}\mathbf{P}^T + \mathbf{E}; \quad \mathbf{Y} = \mathbf{U}\mathbf{Q}^T + \mathbf{F} \quad (7)$$

$$\mathbf{T} = \mathbf{X}\mathbf{W} \underbrace{(\mathbf{P}^T\mathbf{W})^{-1}}_{\triangleq \mathbf{Z}} \quad (8)$$

$$\mathbf{U} = \mathbf{T}\mathbf{B} \quad (9)$$

$$\hat{\mathbf{Y}} = \mathbf{X}\mathbf{Z}\mathbf{B}\mathbf{Q}^T \quad (10)$$

4

where: $\mathbf{X} \in \mathbb{R}^{(N \times n_x)}$, input space; n_x , number of columns in $\mathbf{x}(k)$; N , number of samples in the identification data set; $\mathbf{T} \in \mathbb{R}^{(N \times n_{lv})}$, input scores; n_{lv} , number of latent variables; $\mathbf{P} \in \mathbb{R}^{(n_x \times n_{lv})}$, input loadings; $\mathbf{W} \in \mathbb{R}^{(n_x \times n_{lv})}$, input loadings to get orthogonal scores [15]; $\mathbf{E} \in \mathbb{R}^{(N \times n_x)}$, input residuals; $\mathbf{Y} \in \mathbb{R}^{(N \times n_y)}$, output space; n_y , number of columns in $\mathbf{y}_f(k)$; $\mathbf{U} \in \mathbb{R}^{(N \times n_{lv})}$, output scores; $\mathbf{Q} \in \mathbb{R}^{(n_y \times n_{lv})}$, output loadings; $\mathbf{F} \in \mathbb{R}^{(N \times n_y)}$, output residuals.

2.3. Control methodology

LV-MPC performs optimization in the space of the latent variables, $\Delta \mathbf{t}_d$, and takes the form: [Hereafter the argument k is omitted in the sake of readability.]

$$\min_{\Delta \mathbf{t}_d} \underbrace{\|[\mathbf{r}_f - \hat{\mathbf{y}}_f] \mathbf{W}_y\|_F^2 + \lambda_u \|\Delta \mathbf{x}_{\text{dof}} \mathbf{W}_u\|_F^2}_{\triangleq J_C} \quad s.t. \quad \mathbf{A} \Delta \mathbf{t}_d^T \leq \mathbf{b} \quad (11)$$

where: $\Delta \mathbf{t}_d$, the decision variable in the LV-space; \mathbf{r}_f , the future references defined accordingly to $\hat{\mathbf{y}}_f$; \mathbf{W}_y and \mathbf{W}_u , positive-definite matrices that weigh tracking errors and control increments; λ_u , weighs control increments; $\Delta \mathbf{x}_{\text{dof}}$, increments in the control moves; \mathbf{A} and \mathbf{b} , define linear constraints on the decision variable. Note \mathbf{A} and \mathbf{b} are obtained from the upper, lower and rate limits of the manipulated variables and using some matrices of the controller as explained in Section 2.4 in [6].

To perform the minimization; $\hat{\mathbf{y}}_f$ and $\Delta \mathbf{x}_{\text{dof}}$ are expressed in terms of $\Delta \mathbf{t}_d$:

$$\begin{aligned} \hat{\mathbf{y}}_f &= \mathbf{x}_p^* \bar{\mathbf{S}}_p + \Delta \mathbf{t}_d \bar{\mathbf{S}}_d \\ \Delta \mathbf{x}_{\text{dof}} &= \Delta \mathbf{t}_d \mathbf{M}_{\text{dof}} \end{aligned} \quad (12)$$

where

$$\mathbf{x}_p^* \triangleq \underbrace{[[\mathbf{u}_p \quad \mathbf{u}_{k-n_b}]]}_{\triangleq \mathbf{u}_p^*} \underbrace{[[\mathbf{y}_p \quad \mathbf{y}_{k-n_a-1}]]}_{\triangleq \mathbf{y}_p^*} \quad (13)$$

The control sequence, \mathbf{x}_{dof} , is obtained from $\Delta \mathbf{t}_d$ using the expression:

$$\mathbf{x}_{\text{dof}} = \Delta \mathbf{t}_d \mathbf{M}_{\text{dof}} \Psi_u + \mathbf{u}_{k-1} \Phi_u \quad (14)$$

Provided the receding horizon policy is used, only \mathbf{u}_k contained in \mathbf{x}_{dof} is eventually applied to the process.

3. Validity Indicators for Predictions

Provided performance of any MPC strategy relies on the quality of predictions, validity indicators can be introduced in the MPC problem to ascertain validity of predictions. Two validity indicators commonly used

are Hotelling's T^2 , and residuals in the input space. The former focuses on the regions of the scores and the latter on error of projection from the original space to the latent variable space. These two indicators assume the measured variables follow Gaussian distribution. For non-Gaussian processes, one can consider using instead kernel methods or a combined solution that can tackle with the Gaussian and non-Gaussian term [20]. The two indicators used in this paper, Hotelling's T^2 and residuals in the input space, depend on future moves as well as on past data. If validity indicators contain past data, and past data lays outside the region spanned by the identification data set, validity indicators provide large values regardless of the future trajectory of the MVs. Consequently, there may be no solution of the MVs to keep validity indicators in the valid region because it is the past what causes the indicators to present large values. If past data is neglected however, validity indicators define which future trajectories are acceptable compared to those used for identification. Consequently, the decision of the controller is not constrained by the past, which cannot be changed, but by having acceptable future trajectories of the manipulated variables so that the predictor is not used in extrapolation. Two validity indicators for predictions based on Hotelling's T^2 , and residuals in the input space that neglect past data are defined in this paper.

The former yields:

$$\check{J}_t = \frac{1}{\check{J}_{tmax}} \check{\mathbf{t}} \check{\mathbf{S}}_a^{2^{-1}} \check{\mathbf{t}}^T \quad (15)$$

where $\check{\mathbf{t}}$ is the projection of the input space to the latent variable space neglecting past values; $\check{\mathbf{S}}_a^2$ is a diagonal matrix such that element i is the variance of the score \check{t}_i in the identification data set; and \check{J}_{tmax} is the value of the expression $\check{\mathbf{t}} \check{\mathbf{S}}_a^{2^{-1}} \check{\mathbf{t}}^T$ that includes 95 % of the observations in the identification data set. Provided \check{J}_t is normalized, $\check{J}_t \leq 1$ implies the model is being used in the region in which it has been identified.

The latter can be expressed

$$\check{J}_e = \frac{1}{\check{J}_{emax}} \check{\mathbf{e}} \check{\mathbf{e}}^T \quad (16)$$

where $\check{\mathbf{e}}$ represents the error of projecting the input space to the latent variable space neglecting past values; and \check{J}_{emax} is the value of the expression $\check{\mathbf{e}} \check{\mathbf{e}}^T$ that includes 95 % of the observations in the identification data set. Provided \check{J}_e is normalized, $\check{J}_e \leq 1$ implies the model is being used in the region in which it has been identified.

To include these indices in the controller, both indices need be expressed as a function of $\Delta \mathbf{t}_d$. $\check{J}_t(\Delta \mathbf{t}_d)$ can be derived from its definition in Equation (15), and the expression for $\check{\mathbf{t}}$ in terms of $\Delta \mathbf{t}_d$ provided in

proposition 3.1

$$\begin{aligned}
\check{J}_t(\Delta \mathbf{t}_d) &= \Delta \mathbf{t}_d \check{\mathbf{H}}_t \Delta \mathbf{t}_d^T + 2\check{\mathbf{f}}_t^T \Delta \mathbf{t}_d^T + \mathbf{x}_p^* \frac{\check{\mathbf{N}}_p \mathbf{Z} \check{\mathbf{S}}_a^{2^{-1}} \mathbf{Z}^T \check{\mathbf{N}}_p^T}{\check{J}_{tmax}} \mathbf{x}_p^{*T} \\
\check{\mathbf{H}}_t &\triangleq \frac{\check{\mathbf{N}}_d \mathbf{Z} \check{\mathbf{S}}_a^{2^{-1}} \mathbf{Z}^T \check{\mathbf{N}}_d^T}{\check{J}_{tmax}} \\
\check{\mathbf{f}}_t^T &\triangleq \frac{\mathbf{x}_p^* \check{\mathbf{N}}_p \mathbf{Z} \check{\mathbf{S}}_a^{2^{-1}} \mathbf{Z}^T \check{\mathbf{N}}_d^T}{\check{J}_{tmax}}
\end{aligned} \tag{17}$$

$\check{J}_e(\Delta \mathbf{t}_d)$ can be derived from its definition in Equation (16), and the expression for $\check{\mathbf{e}}$ in terms of $\Delta \mathbf{t}_d$ provided in proposition 3.2

$$\begin{aligned}
\check{J}_e(\Delta \mathbf{t}_d) &= \Delta \mathbf{t}_d \check{\mathbf{H}}_e \Delta \mathbf{t}_d^T + 2\check{\mathbf{f}}_e^T \Delta \mathbf{t}_d^T + \mathbf{x}_p^* \frac{\check{\mathbf{E}}_p \check{\mathbf{E}}_p^T}{\check{J}_{emax}} \mathbf{x}_p^{*T} \\
\check{\mathbf{H}}_e &\triangleq \frac{\check{\mathbf{E}}_d \check{\mathbf{E}}_d^T}{\check{J}_{emax}} \\
\check{\mathbf{f}}_e^T &\triangleq \frac{\mathbf{x}_p^* \check{\mathbf{E}}_p \check{\mathbf{E}}_d^T}{\check{J}_{emax}}
\end{aligned} \tag{18}$$

Proposition 3.1. $\check{\mathbf{t}} = \mathbf{x}_p^* \check{\mathbf{N}}_p \mathbf{Z} + \Delta \mathbf{t}_d \check{\mathbf{N}}_d \mathbf{Z}$

Proof From Equations (8) and (1)

$$\mathbf{t} = \underbrace{[\mathbf{x}_p \quad \mathbf{x}_f \quad \mathbf{x}_{dof}]}_{\mathbf{x}} \mathbf{Z}$$

$\check{\mathbf{t}}$ is defined forcing past data to be zero

$$\check{\mathbf{t}} \triangleq \underbrace{[\mathbf{0} \quad \mathbf{x}_f \quad \mathbf{x}_{dof}]}_{\triangleq \check{\mathbf{x}}} \mathbf{Z} \tag{19}$$

where $\mathbf{0}$ is a vector of zeros with the same dimensions of \mathbf{x}_p .

Provided \mathbf{u}_{k+i} is set to \mathbf{u}_{k+n_u-1} for $i \in [n_u, n_f - 1]$, \mathbf{x}_f can be expressed:

$$\mathbf{x}_f = \mathbf{x}_{dof} \underbrace{\begin{bmatrix} \mathbf{I}_{n_i} & \dots & \mathbf{I}_{n_i} \\ \mathbf{0}_{(n_u-1)n_i \times (n_f-n_u)n_i} \end{bmatrix}}_{\triangleq \Gamma} \tag{20}$$

then taking matrices $\mathbf{0}$ and \mathbf{I} of appropriate dimensions,

$$\check{\mathbf{x}} = \mathbf{x}_{dof} [\mathbf{0} \quad \Gamma \quad \mathbf{I}]$$

From the definition of \mathbf{x}_p^* in Equation (13), and the expression for \mathbf{x}_{dof} in Equation (14):

$$\check{\mathbf{x}} = \mathbf{x}_p^* \check{\mathbf{N}}_p + \Delta \mathbf{t}_d \check{\mathbf{N}}_d \tag{21}$$

where

$$\begin{aligned}\check{\mathbf{N}}_p &\triangleq \begin{bmatrix} \Phi_u[\mathbf{0} \ \Gamma \ \mathbf{I}] \\ \mathbf{0} \end{bmatrix} \\ \check{\mathbf{N}}_d &\triangleq \mathbf{M}_{\text{dof}} \Psi_u[\mathbf{0} \ \Gamma \ \mathbf{I}]\end{aligned}$$

thus,

$$\check{\mathbf{t}} = \mathbf{x}_p^* \check{\mathbf{N}}_p \mathbf{Z} + \Delta t_d \check{\mathbf{N}}_d \mathbf{Z}. \quad \square$$

Proposition 3.2. $\check{\mathbf{e}} = \mathbf{x}_p^* \check{\mathbf{E}}_p + \Delta t_d \check{\mathbf{E}}_d$

Proof From Equation (7)

$$\mathbf{X} = \mathbf{TP}^T + \mathbf{E}; \quad \Rightarrow \quad \mathbf{e} = \mathbf{x} - \mathbf{tP}^T$$

which neglecting past data as in Equation (19) can be expressed:

$$\check{\mathbf{e}} = \check{\mathbf{x}} - \check{\mathbf{t}}\mathbf{P}^T$$

Substituting $\check{\mathbf{t}}$ in from Equation (19)

$$\check{\mathbf{e}} = \check{\mathbf{x}}(\mathbf{I} - \mathbf{ZP}^T)$$

Substituting in from Equation (21)

$$\check{\mathbf{e}} = \mathbf{x}_p^* \underbrace{\check{\mathbf{N}}_p(\mathbf{I} - \mathbf{ZP}^T)}_{\triangleq \check{\mathbf{E}}_p} + \Delta t_d \underbrace{\check{\mathbf{N}}_d(\mathbf{I} - \mathbf{ZP}^T)}_{\triangleq \check{\mathbf{E}}_d}$$

thus

$$\check{\mathbf{e}} = \mathbf{x}_p^* \check{\mathbf{E}}_p + \Delta t_d \check{\mathbf{E}}_d. \quad \square$$

4. Add constraints on Validity Indicators

There are two options to consider validity indicators for predictions in the LV-MPC problem: soft constraints or hard constraints. The soft constraints approach is used in [6] in which validity indicators that consider past data are weighed in the control cost function. The main advantage of the soft constraints approach is it is easier to implement, but yields the drawback that there is no tuning strategy to ascertain validity of predictions in any situation. In this paper validity indicators for predictions are included as hard constraints in the LV-MPC formulation. Note that if validity indicators are forced to be below 1, no extrapolation is allowed; however, as predictions are expected to degrade gradually as the process moves away from the identification envelope, one can leave some room for extrapolation by choosing a value above 1 for the

threshold. Then the hard constraints approach defined in this paper adds some complexity, but ensures validity of predictions providing a tool to control how much extrapolation is allowed.

The minimization problem in Equation (11) can be augmented with constraints on \check{J}_t and \check{J}_e .

$$\min_{\Delta \mathbf{t}_d} J_C \quad s.t. \quad \begin{cases} \mathbf{A} \Delta \mathbf{t}_d^T \leq \mathbf{b} \\ \check{J}_t \leq 1 \\ \check{J}_e \leq 1 \end{cases} \quad (22)$$

Note from Equations (17) and (18) that \check{J}_t and \check{J}_e depend quadratically on $\Delta \mathbf{t}_d$, and so the problem in Equation (22) is a QCQP.

In a QCQP we minimize a convex quadratic function over a feasible region that is the intersection of ellipsoids [16]. In a QP however, we minimize a convex quadratic function over a feasible region that is the intersection of hyperplanes. A mean to simplify the QCQP is to transform it into a QP by bounding the ellipsoids by hyperplanes provided quadratic constraints are convex. Such hyperplanes are obtained by linearising the ellipsoids at some points of interest. Such an approach provides a solution for the first iteration and improves it in terms of satisfying quadratic constraints as the algorithm evolves. The advantage of this approach is it can be stopped before it converges, if a solution is needed at that time as can happen in real-time implementations. However, if there is enough time, the algorithm can converge and provide a solution that ascertains quadratic constraints.

Given the set of hyperplanes $\mathbf{A}_t \Delta \mathbf{t}_d^T \leq \mathbf{b}_t$ that bounds quadratic constraint $\check{J}_t \leq 1$, and the set of hyperplanes $\mathbf{A}_e \Delta \mathbf{t}_d^T \leq \mathbf{b}_e$ that bounds quadratic constraint $\check{J}_e \leq 1$, the QCQP in Equation (22) is reformulated:

$$\min_{\Delta \mathbf{t}_d} J_C \quad s.t. \quad \begin{cases} \mathbf{A} \Delta \mathbf{t}_d^T \leq \mathbf{b} \\ \begin{bmatrix} \mathbf{A}_t \\ \mathbf{A}_e \end{bmatrix} \Delta \mathbf{t}_d^T \leq \begin{bmatrix} \mathbf{b}_t \\ \mathbf{b}_e \end{bmatrix} \end{cases} \quad (23)$$

\mathbf{A}_t , \mathbf{b}_t , \mathbf{A}_e , and \mathbf{b}_e are needed to solve the problem in Equation (23), however, they are initially unknown. The problem in Equation (23) can be solved by means of the following iterative procedure, where $\Delta \mathbf{t}_{d_i}$ stands for $\Delta \mathbf{t}_d$ at iteration i .

1. \mathbf{A}_t , \mathbf{b}_t , \mathbf{A}_e , and \mathbf{b}_e are initialized empty,
2. $\Delta \mathbf{t}_{d_i}$ comes from solving the QP in Equation (23)
3. the algorithm finishes if $\Delta \mathbf{t}_{d_i}$ satisfies both quadratic constraints: $\check{J}_t \leq 1$ and $\check{J}_e \leq 1$
4. if $\check{J}_t \leq 1$ does not hold; \check{J}_t is linearised, and \mathbf{A}_t , \mathbf{b}_t are augmented with the linearised constraint
5. if $\check{J}_e \leq 1$ does not hold; \check{J}_e is linearised, and \mathbf{A}_e , \mathbf{b}_e are augmented with the linearised constraint
6. go to step 2

Linearisation of the quadratic constraints on steps 4 and 5 in the above procedure is implemented taking the first order Taylor approximation of the quadratic constraints. Two approaches depending on which point is used for linearisation are considered:¹

- (I) Linearise $\check{J}_t \leq 1$ at the current solution $\Delta \mathbf{t}_{d_i}$,
- (II) Linearise $\check{J}_t \leq 1$ at $\Delta \mathbf{t}_{d_{ti}}$. $\Delta \mathbf{t}_{d_{ti}}$ is defined such that $\check{J}_t(\Delta \mathbf{t}_{d_{ti}}) = 1$, and it is aligned with the current solution $\Delta \mathbf{t}_{d_i}$ and $\Delta \mathbf{t}_{d_t}$. Where $\Delta \mathbf{t}_{d_t}$ minimizes \check{J}_t in Equation (17) which can be expressed $\Delta \mathbf{t}_{d_t} = -\mathbf{f}_t^T \mathbf{H}_t^{-1}$. The expression for $\Delta \mathbf{t}_{d_{ti}}$ is derived in proposition 4.1.

The First order Taylor approximation of the quadratic constraint $\check{J}_t \leq 1$ at iteration i is derived in proposition 4.3

$$\mathbf{A}_{t_i} \Delta \mathbf{t}_d^T \leq \mathbf{B}_{t_i}.$$

In the sake of clarity and to compare both linearisation approaches, the following two-dimensional example is considered:

$$J_C = \Delta \mathbf{t}_d \begin{bmatrix} 0.1 & 0.1 \\ 0.1 & 0.2 \end{bmatrix} \Delta \mathbf{t}_d^T + 2[-0.2 \quad 0] \Delta \mathbf{t}_d^T$$

$$\check{J}_t = \Delta \mathbf{t}_d \begin{bmatrix} 0.1 & 0 \\ 0 & 0.01 \end{bmatrix} \Delta \mathbf{t}_d^T + 2[0.05 \quad 0] \Delta \mathbf{t}_d^T + 0.8$$

In Figures 1 and 2: the contour plot of the cost function J_C is in grey; the area inside the ellipse satisfies constraint $\check{J}_t \leq 1$; $\Delta \mathbf{t}_{d_i}$ is the solution of the QP problem with the current constraints; $\Delta \mathbf{t}_{d_t}$ is the minimum of \check{J}_t ; and $\Delta \mathbf{t}_{d_{ti}}$ is aligned with $\Delta \mathbf{t}_{d_i}$ and $\Delta \mathbf{t}_{d_t}$ and intersects with the boundary of the quadratic constraint $\check{J}_t(\Delta \mathbf{t}_{d_{ti}}) = 1$.

Constraint $\check{J}_t \leq 1$ is linearised at $\Delta \mathbf{t}_{d_i}$ and represented in thick line in Figure 1, whereas in Figure 2 it is linearised at $\Delta \mathbf{t}_{d_{ti}}$. From those figures, the second approach linearises the constraint at the boundary which is the area of interest, and consequently the algorithm converges faster to a solution that satisfies constraints.

Summing up, this section defines an iterative procedure to solve the resulting QCQP obtained when adding validity constraints into the LV-MPC problem. The procedure is iterative and at each iteration quadratic constraints are linearised and a QP is solved.

¹Linearisation of the quadratic constraint $\check{J}_t \leq 1$ is explained, but the same procedure applies to $\check{J}_e \leq 1$.

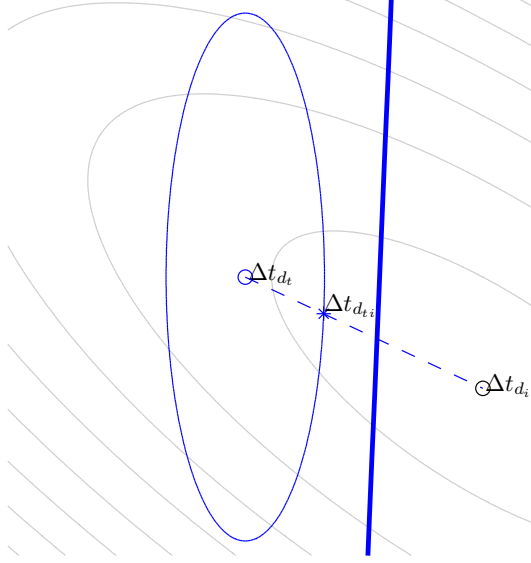


Figure 1: Linearise at $\Delta \mathbf{t}_{d_i}$

Proposition 4.1. $\Delta \mathbf{t}_{d_{ti}}$ such that $\check{J}_t(\Delta \mathbf{t}_{d_{ti}}) = 1$, and it is aligned with the current solution $\Delta \mathbf{t}_{d_i}$ and $\Delta \mathbf{t}_{d_t}$ is obtained:

$$\Delta \mathbf{t}_{d_{ti}} = \Delta \mathbf{t}_{d_t} + \check{\gamma}_t(\Delta \mathbf{t}_{d_i} - \Delta \mathbf{t}_{d_t})$$

Proof $\Delta \mathbf{t}_{d_{ti}}$ is a point which satisfies:

- $\Delta \mathbf{t}_{d_{ti}}$ is aligned with $\Delta \mathbf{t}_{d_i}$ and $\Delta \mathbf{t}_{d_t}$
- $\Delta \mathbf{t}_{d_{ti}}$ is in-between $\Delta \mathbf{t}_{d_i}$ and $\Delta \mathbf{t}_{d_t}$
- $\check{J}_t(\Delta \mathbf{t}_{d_{ti}}) = 1$

The first requirement can be expressed:

$$\Delta \mathbf{t}_d(\gamma_t) = \Delta \mathbf{t}_{d_t} + \gamma_t(\Delta \mathbf{t}_{d_i} - \Delta \mathbf{t}_{d_t})$$

where $\gamma_t \in \mathbb{R}$. For the second requirement to hold $\gamma_t \in [0, 1]$. Substituting $\Delta \mathbf{t}_d$ in proposition 3.1

$$\check{\mathbf{t}}(\gamma_t) = \mathbf{x}_p^* \check{\mathbf{N}}_p \mathbf{Z} + \underbrace{(\Delta \mathbf{t}_{d_t} + \gamma_t(\Delta \mathbf{t}_{d_i} - \Delta \mathbf{t}_{d_t}))}_{\Delta \mathbf{t}_d} \check{\mathbf{N}}_d \mathbf{Z}$$

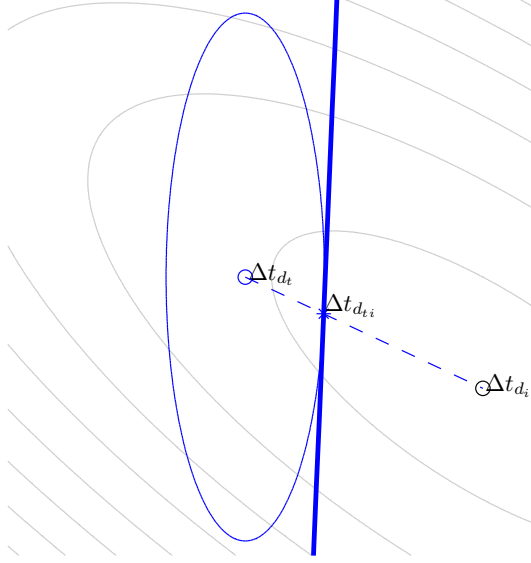


Figure 2: Linearise at $\Delta \mathbf{t}_{d_i}$

which yields

$$\check{\mathbf{t}}(\gamma_t) = \underbrace{\mathbf{x}_p^* \check{\mathbf{N}}_p \mathbf{Z} + \Delta \mathbf{t}_{d_i} \check{\mathbf{N}}_d \mathbf{Z}}_{\triangleq \check{\mathbf{M}}_t} + \gamma_t \underbrace{(\Delta \mathbf{t}_{d_i} - \Delta \mathbf{t}_{d_t}) \check{\mathbf{N}}_d \mathbf{Z}}_{\triangleq \check{\mathbf{N}}_t}$$

Substituting $\check{\mathbf{t}}(\gamma_t)$ in Equation (15)

$$\begin{aligned} \check{J}_t(\gamma_t) &= \frac{(\check{\mathbf{M}}_t + \gamma_t \check{\mathbf{N}}_t) \check{\mathbf{S}}_a^{2^{-1}} (\check{\mathbf{M}}_t^T + \gamma_t \check{\mathbf{N}}_t^T)}{\check{J}_{tmax}} \\ &= \underbrace{\frac{\check{\mathbf{N}}_t \check{\mathbf{S}}_a^{2^{-1}} \check{\mathbf{N}}_t^T}{\check{J}_{tmax}}}_{\triangleq a_t} \gamma_t^2 + \underbrace{\frac{2\check{\mathbf{M}}_t \check{\mathbf{S}}_a^{2^{-1}} \check{\mathbf{N}}_t^T}{\check{J}_{tmax}}}_{\triangleq b_t} \gamma_t + \underbrace{\frac{\check{\mathbf{M}}_t \check{\mathbf{S}}_a^{2^{-1}} \check{\mathbf{M}}_t^T}{\check{J}_{tmax}}}_{\triangleq c_t} \end{aligned}$$

The third requirement can be expressed

$$\check{J}_t(\bar{\gamma}_t) = 1$$

where $\bar{\gamma}_t$ comes from solving the above second order equation

$$\bar{\gamma}_t = \frac{-b_t \pm \sqrt{b_t^2 - 4a_t(c_t - 1)}}{2a_t}.$$

Provided \check{J}_t is symmetric to its minimum; and both $\check{J}_t(\bar{\gamma}_t)$ are aligned with the point that minimizes \check{J}_t , the absolute value of the two solutions in the previous equation are equal. Since we are only interested in

values of $\gamma_t \in [0, 1]$ we take the positive solution. Note that in case $\bar{\gamma}_t > 1$, the current solution $\Delta \mathbf{t}_{d_i}$ already satisfies the constraint and no linearisation of the quadratic constraint is needed. Consequently $\Delta \mathbf{t}_{d_{ti}}$ need be computed only if $\bar{\gamma}_t \leq 1$

$$\tilde{\gamma}_t = \frac{-b_t + \sqrt{b_t^2 - 4a_t(c_t - 1)}}{2a_t}.$$

and $\Delta \mathbf{t}_{d_{ti}}$ can be expressed

$$\Delta \mathbf{t}_{d_{ti}} = \Delta \mathbf{t}_{d_t} + \tilde{\gamma}_t(\Delta \mathbf{t}_{d_i} - \Delta \mathbf{t}_{d_t}). \quad \square$$

Proposition 4.2. $\Delta \mathbf{t}_{d_{ei}}$ such that $\check{J}_e(\Delta \mathbf{t}_{d_{ei}}) = 1$, and it is aligned with the current solution $\Delta \mathbf{t}_{d_i}$ and $\Delta \mathbf{t}_{d_e}$ is obtained:

$$\Delta \mathbf{t}_{d_{ei}} = \Delta \mathbf{t}_{d_e} + \tilde{\gamma}_e(\Delta \mathbf{t}_{d_i} - \Delta \mathbf{t}_{d_e})$$

Proof $\Delta \mathbf{t}_{d_{ei}}$ is a point which satisfies:

- $\Delta \mathbf{t}_{d_{ei}}$ is aligned with $\Delta \mathbf{t}_{d_i}$ and $\Delta \mathbf{t}_{d_e}$
- $\Delta \mathbf{t}_{d_{ei}}$ is in-between $\Delta \mathbf{t}_{d_i}$ and $\Delta \mathbf{t}_{d_e}$
- $\check{J}_e(\Delta \mathbf{t}_{d_{ei}}) = 1$

The first requirement can be expressed:

$$\Delta \mathbf{t}_d(\gamma_e) = \Delta \mathbf{t}_{d_e} + \gamma_e(\Delta \mathbf{t}_{d_i} - \Delta \mathbf{t}_{d_e})$$

where $\gamma_e \in \mathbb{R}$. For the second requirement to hold $\gamma_e \in [0, 1]$. Substituting $\Delta \mathbf{t}_d$ in proposition 3.2

$$\check{\mathbf{e}}(\gamma_e) = \mathbf{x}_p^* \check{\mathbf{E}}_p + \underbrace{(\Delta \mathbf{t}_{d_e} + \gamma_e(\Delta \mathbf{t}_{d_i} - \Delta \mathbf{t}_{d_e}))}_{\Delta \mathbf{t}_d} \check{\mathbf{E}}_d$$

which yields

$$\check{\mathbf{e}}(\gamma_e) = \underbrace{\mathbf{x}_p^* \check{\mathbf{E}}_p + \Delta \mathbf{t}_{d_e} \check{\mathbf{E}}_d}_{\triangleq \check{M}_e} + \gamma_e \underbrace{(\Delta \mathbf{t}_{d_i} - \Delta \mathbf{t}_{d_e}) \check{\mathbf{E}}_d}_{\triangleq \check{N}_e}$$

Substituting $\check{\mathbf{e}}(\gamma_e)$ in Equation (16)

$$\begin{aligned} \check{J}_e(\gamma_e) &= \frac{(\check{M}_e + \gamma_e \check{N}_e)(\check{M}_e^T + \gamma_e \check{N}_e^T)}{\check{J}_{emax}} \\ &= \frac{\check{N}_e \check{N}_e^T}{\check{J}_{emax}} \gamma_e^2 + \frac{2\check{M}_e \check{N}_e^T}{\check{J}_{emax}} \gamma_e + \frac{\check{M}_e \check{M}_e^T}{\check{J}_{emax}} \\ &\quad \underbrace{\hspace{1.5cm}}_{\triangleq a_e} \quad \underbrace{\hspace{1.5cm}}_{\triangleq b_e} \quad \underbrace{\hspace{1.5cm}}_{\triangleq c_e} \end{aligned}$$

The third requirement can be expressed

$$\check{J}_e(\bar{\gamma}_e) = 1$$

where $\bar{\gamma}_e$ comes from solving the above second order equation

$$\bar{\gamma}_e = \frac{-b_e \pm \sqrt{b_e^2 - 4a_e(c_e - 1)}}{2a_e}.$$

Provided \check{J}_e is symmetric to its minimum; and both $\check{J}_e(\bar{\gamma}_e)$ are aligned with the point that minimizes \check{J}_e , the absolute value of the two solutions in the previous equation are equal. Since we are only interested in values of $\gamma_e \in [0, 1]$ we take the positive solution. Note that in case $\bar{\gamma}_e > 1$, the current solution $\Delta \mathbf{t}_{d_i}$ already satisfies the constraint and no linearisation of the quadratic constraint is needed. Consequently $\Delta \mathbf{t}_{d_{ei}}$ need be computed only if $\bar{\gamma}_e \leq 1$

$$\check{\gamma}_e = \frac{-b_e + \sqrt{b_e^2 - 4a_e(c_e - 1)}}{2a_e}.$$

and $\Delta \mathbf{t}_{d_{ei}}$ can be expressed

$$\Delta \mathbf{t}_{d_{ei}} = \Delta \mathbf{t}_{d_e} + \check{\gamma}_e(\Delta \mathbf{t}_{d_i} - \Delta \mathbf{t}_{d_e}). \quad \square$$

Proposition 4.3. *The first-order Taylor approximation of the quadratic constraint $\check{J}_t \leq 1$ at a point β can be expressed*

$$\mathbf{A}_{t_i} \Delta \mathbf{t}_d^T \leq \mathbf{B}_{t_i}$$

Proof The first-order Taylor approximation of the quadratic constraint $\check{J}_t \leq 1$ at a point β

$$\left. \frac{\partial \check{J}_t}{\partial \Delta \mathbf{t}_d} \right|_{\beta} (\Delta \mathbf{t}_d - \beta) + \check{J}_t(\beta) \leq 1 \quad (24)$$

$\beta = \Delta \mathbf{t}_{d_i}$ or $\beta = \Delta \mathbf{t}_{d_{ei}}$ depending on which linearisation point is selected. The first derivative of \check{J}_t in Equation (17) with respect to $\Delta \mathbf{t}_d$

$$\frac{\partial \check{J}_t}{\partial \Delta \mathbf{t}_d} = 2\Delta \mathbf{t}_d \mathbf{H}_t + 2\mathbf{f}_t^T$$

then

$$\left. \frac{\partial \check{J}_t}{\partial \Delta \mathbf{t}_d} \right|_{\beta} = 2\beta \mathbf{H}_t + 2\mathbf{f}_t^T.$$

Reorganising terms in Equation (24)

$$\underbrace{\left. \frac{\partial \check{J}_t}{\partial \Delta \mathbf{t}_d} \right|_{\beta}}_{\triangleq \mathbf{A}_{t_i}} \Delta \mathbf{t}_d \leq \underbrace{1 - \check{J}_t(\beta) + \left. \frac{\partial \check{J}_t}{\partial \Delta \mathbf{t}_d} \right|_{\beta} \beta}_{\triangleq \mathbf{B}_{t_i}}$$

Note that for $\beta = \Delta \mathbf{t}_{d_{ei}}$, $\check{J}_t(\beta) = \check{J}_t(\Delta \mathbf{t}_{d_{ei}}) = 1$ thus

$$\mathbf{B}_{t_i} = \left. \frac{\partial \check{J}_t}{\partial \Delta \mathbf{t}_d} \right|_{\beta} \beta. \quad \square$$

Proposition 4.4. *The first-order Taylor approximation of the quadratic constraint $\check{J}_e \leq 1$ at a point β can be expressed*

$$\mathbf{A}_{e_i} \Delta \mathbf{t}_d^T \leq \mathbf{B}_{e_i}$$

Proof The first-order Taylor approximation of the quadratic constraint $\check{J}_e \leq 1$ at a point β can be expressed

$$\left. \frac{\partial \check{J}_e}{\partial \Delta \mathbf{t}_d} \right|_{\beta} (\Delta \mathbf{t}_d - \beta) + \check{J}_e(\beta) \leq 1 \quad (25)$$

$\beta = \Delta \mathbf{t}_{d_i}$ or $\beta = \Delta \mathbf{t}_{d_{ei}}$ depending on which linearisation point is selected. The first derivative of \check{J}_e in Equation (18) with respect to $\Delta \mathbf{t}_d$

$$\frac{\partial \check{J}_e}{\partial \Delta \mathbf{t}_d} = 2\Delta \mathbf{t}_d \mathbf{H}_e + 2\mathbf{f}_e^T$$

then

$$\left. \frac{\partial \check{J}_e}{\partial \Delta \mathbf{t}_d} \right|_{\beta} = 2\beta \mathbf{H}_e + 2\mathbf{f}_e^T.$$

Reorganising terms in Equation (25)

$$\underbrace{\left. \frac{\partial \check{J}_e}{\partial \Delta \mathbf{t}_d} \right|_{\beta}}_{\triangleq \mathbf{A}_{e_i}} \Delta \mathbf{t}_d \leq \underbrace{1 - \check{J}_e(\beta) + \left. \frac{\partial \check{J}_e}{\partial \Delta \mathbf{t}_d} \right|_{\beta} \beta}_{\triangleq \mathbf{B}_{e_i}}$$

Note that if $\beta = \Delta \mathbf{t}_{d_{ei}}$, then $\check{J}_e(\beta) = 1$ and

$$\mathbf{B}_{e_i} = \left. \frac{\partial \check{J}_e}{\partial \Delta \mathbf{t}_d} \right|_{\beta} \beta. \quad \square$$

5. Simulation results and discussion

In this section the model of a boiler is controlled by means of

DM Traditional data-driven MPC approach with no validity indicators [17]

LV-MPC The methodology proposed in [6] with no validity indicators

LV-MPC-cons LV-MPC with constraints on \bar{J}_t and \bar{J}_e to ensure model validity. These indicators are equivalent to \check{J}_t and \check{J}_e defined in section 3, but past is not neglected.

LV-MPC-cons-neg LV-MPC with constraints on \check{J}_t and \check{J}_e to ensure model validity.

In this section first a description of the process is provided; second control parameters are set; third the predictor is obtained from data; and finally two control scenarios are considered: normal operation, and large changes in set points and disturbance.

5.1. Process description

The process to control is the nonlinear model of a Boiler proposed by Pellegrinetti and Bentsman [18]. The model has been developed in Simulink² including some changes: several coefficients have been slightly modified, restricted ranges for the inputs and outputs have been selected and normalized in percentage. However, the following main features of the model have been preserved:

- It has a relatively low complexity while faithfully capturing the essential plant dynamics and its nonlinearities over a wide operating range.
- The model is control oriented in that the manipulated variables, the controlled variables and the significant disturbance are explicitly shown.
- The model is realistic in that the constraints on the manipulated variables are known, and the measurement noise and time delays are present on the outputs.

The variables in the process and their working points are:

- MVs:
 - u_1 : Fuel flow; range [0 100]; operating point 35.21 %
 - u_2 : Water flow; range [0 100]; operating point 57.57 %
- Disturbance:
 - m_1 : load level; range [0 100]; operating point 46.36 %
- CVs:
 - y_1 : Steam pressure; range [0 100]; operating point 60 %
 - y_2 : Water level; range [0 100]; operating point 50 %

The main control difficulties in this multivariable process are caused by the coupling, the non-minimum phase, the integration and the load disturbance.

²<http://www.dia.uned.es/~fmorilla/benchmarkPID2012/>

5.2. Control parameters

The sampling time is defined from the step response of the process to a step of 10% in the inputs (Figures 3 and 4) and disturbance (Figure 5). From the dynamic response of both outputs, the time constant of the process is about 50 seconds, and T_s is set as the time constant divided by 10, then $T_s = 5$ s.

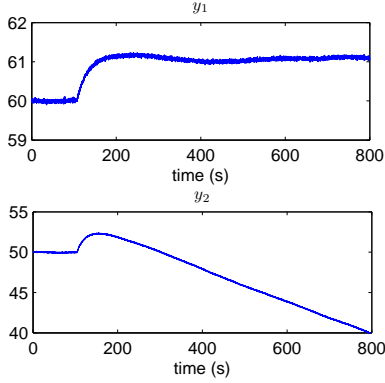


Figure 3: Step in u_1

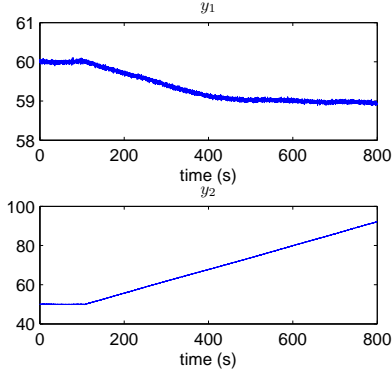


Figure 4: Step in u_2

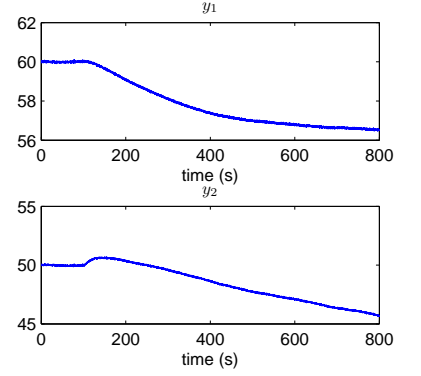


Figure 5: Step in m_1

It is convenient in MPC to choose n_u and n_f such that $n_f - n_u$ is greater than or equal to the process settling time towards changes in the MVs. From Figure 4, settling time for output y_1 is about 300 seconds. y_2 has an integrator hence it does not settle, however it moves at a constant rate 100 seconds after the step. Consequently, $n_f - n_u$ is set to 300 seconds, and for $T_s = 5$ s

$$n_f - n_u = \frac{300}{5} = 60 \text{ samples.}$$

According to the experience of the authors, n_u can be set as half the value set for $n_f - n_u$, which in this case yields $n_u = 30$. However, from Figure 5, the settling time of y_1 to a change in m_1 is about 600 seconds, then n_f should be at least 600 seconds:

$$n_f = \frac{600}{5} = 120 \text{ samples}$$

then

$$n_f - n_u = 60 \Rightarrow n_u = n_f - 60 = 120 - 60 = 60 \text{ samples.}$$

Constraints are defined for the MVs and their rate:

- $0 \leq u_i \leq 100, \quad \forall i \in [1, 2]$
- $|\Delta u_i| \leq 1\%/sec, \quad \forall i \in [1, 2]$

Future references are assumed unknown,

$$\mathbf{r}_{k+i} = \mathbf{r}_{k+1}, \quad \forall i \in [1, n_f]$$

The weight of the control moves is set so that a fast response is obtained

$$\lambda_u = 1$$

5.3. Identification

The identification and validation data sets in Figure 6 are obtained in closed-loop. According to [19] closed-loop tests have many advantages over openloop tests. A closed-loop test is easy to carry out, will reduce the disturbance to process operation, and will excite more control-relevant information content of the underlying process. The continuous blue plots represent the identification data set, and the discontinuous green plots represent the validation data set. To obtain the identification and validation data sets the process is controlled using two PID controllers. The set points of the CVs are moved around the working point; steps of 10% amplitude are added to m_1 ; and steps of 20% amplitude are added to the MVs.

Prior to identification, the set point is removed from the MVs and the CVs. m_1 is not considered in the model. To decide the order of the model, n_a and n_b are swept and two indicators are evaluated for the validation data set. The two indicators are the sum of squared prediction errors one-step ahead \bar{J}_{OSAPI} , and multi-step ahead \bar{J}_{LRPI} , both of them normalized to the number of quadratic terms to sum:

$$\bar{J}_{\text{OSAPI}} = \frac{1}{Nn_o} \sum_{k=1}^N \|\mathbf{y}_k - \hat{\mathbf{y}}_k\|_F^2; \quad \bar{J}_{\text{LRPI}} = \frac{1}{Nn_o n_f} \sum_{k=1}^N \|\mathbf{y}_f(k) - \hat{\mathbf{y}}_f(k)\|_F^2.$$

Figure 7 plots the values of \bar{J}_{OSAPI} and \bar{J}_{LRPI} for different values of n , being $n_a = n$ and $n_b = n$. From Figure 7(a) $n \geq 4$, and from Figure 7(b) $2 \leq n \leq 4$, then a fourth order linear model is used to approximate the nonlinear process: $n_a = n_b = 4$.

In this section two models are fit: the LV-MPC model and the DM model. Both models are fourth order linear models as defined in Section 2.1, but the DM model is fit using Least Squares and the LV-MPC model is a PLS model (Section 2.2). The next step is to choose n_{lv} for the LV-MPC model. n_{lv} can take any value in-between 1 and the number of columns in $\mathbf{x}(k)$, which in this example yields $(n_b - 1)n_i + n_a n_o + n_f n_i = 254$ columns in $\mathbf{x}(k)$. Consequently n_{lv} can take any value in-between 1 and 254, however, the controller has $n_u n_i = 120$ d.o.f., then n_{lv} is to be swept in-between 1 and 120.

Figure 8 plots in continuous blue line $\bar{J}_{\text{OSAPI}}(n)$ and $\bar{J}_{\text{LRPI}}(n)$ for the LV-MPC model, and in discontinuous black line $\bar{J}_{\text{OSAPI}}(n)$ and $\bar{J}_{\text{LRPI}}(n)$ for the DM model. From Figure 8(a), $n_{lv} \geq 80$. From Figure 8(b),

$40 \leq n_{lv} \leq 60$ or $n_{lv} \geq 100$. Then³

$$n_{lv} = 100.$$

Predictive performance of the two models obtained is tested performing predictions for the validation data set. Figures 9 and 10 contain one-step ahead predictions, predictions in the far prediction horizon, and the coefficient of determination R^2 evaluated for predictions from $k + 1$ up to $k + n_f$. Note the LV-MPC model contains 100 latent variables out of the 254 columns in the input vector of the model, but still performs as the DM model. One-step ahead predictions are almost exact for both outputs, then R^2 in the near horizon reaches 1. Predictions at $k + n_f$ slightly differ from the real output, but R^2 is always above 0.8, then the predictor is considered to successfully approximate the process in the prediction window.

³Note that, as previously stated, the number of columns in $\mathbf{x}(k)$ is 254, and $n_{lv} = 100$, thus a reduction of 60% in the number of variables has been performed.

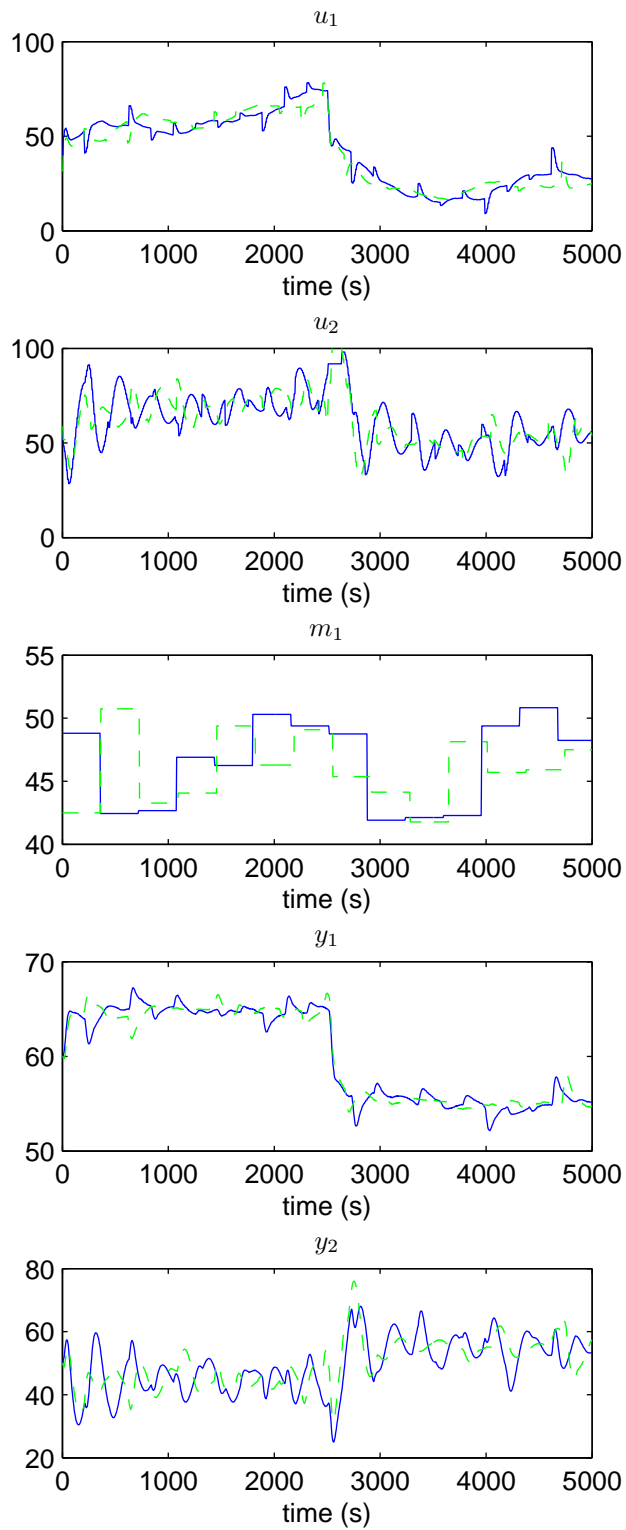


Figure 6: Identification and validation data sets

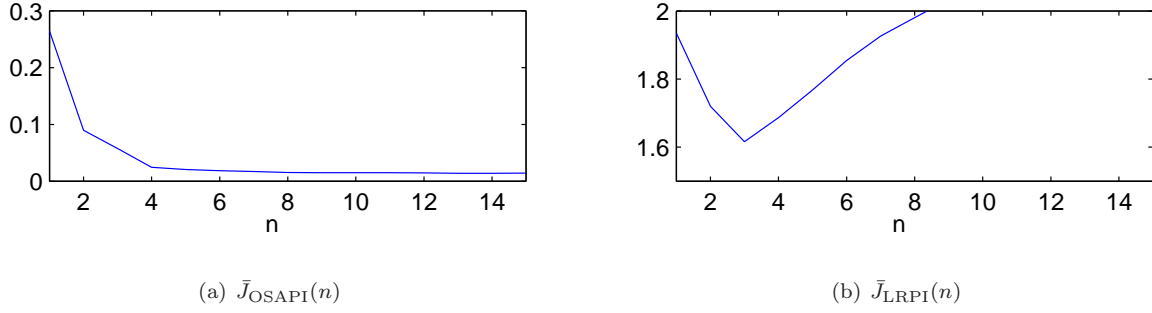


Figure 7: Identification Indicators versus n .

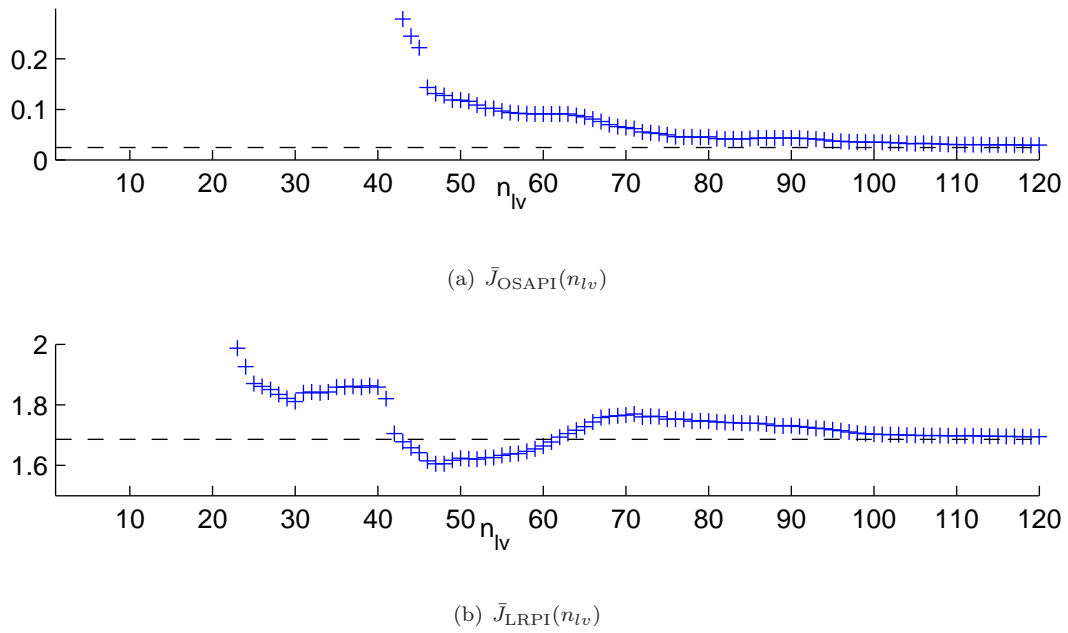


Figure 8: Identification Indicators versus n_{lv} . LV-MPC model (+ symbol) and DM model (dashed-line). Note in the DM model there is no n_{lv} , then a constant value for both indicators is provided.

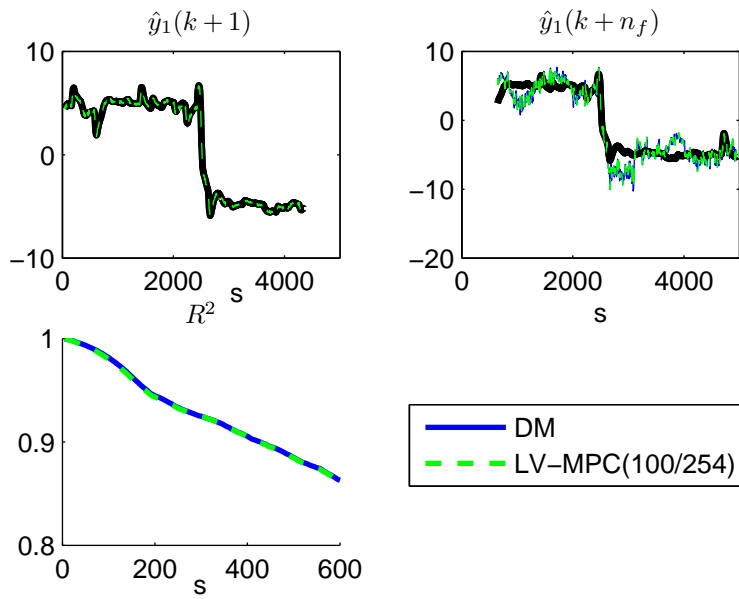


Figure 9: Validation results for y_1 removing the working point.

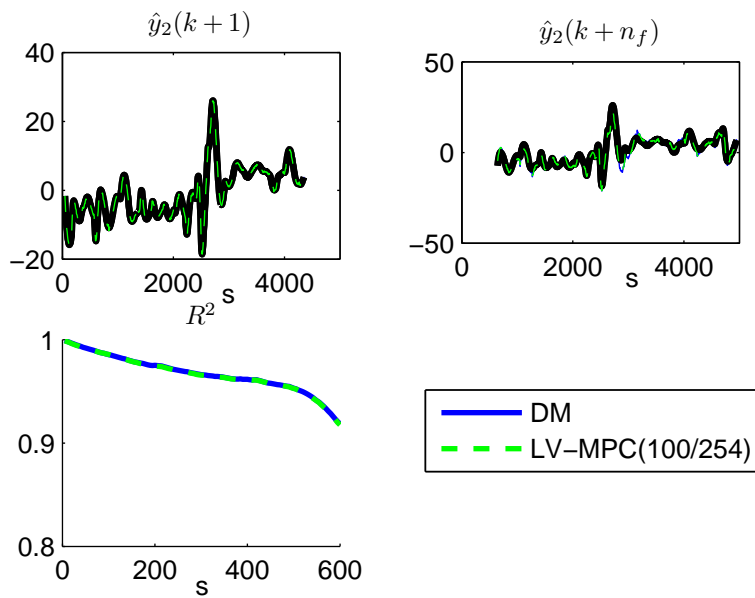


Figure 10: Validation results for y_2 removing the working point.

5.4. Control results: normal operation

The different control strategies are tested in a situation similar to the identification experiment. Steps are applied to the set points of the CVs. From Figure 11, LV-MPC strategies slightly outperform DM. Note in LV-MPC the controller has 100 d.o.f., whilst in DM there are $n_u n_i = 120$ d.o.f.. LV-MPC equals LV-MPC-cons-neg provided quadratic constraints neglecting past data are not active for large periods of time (Figure 13). In LV-MPC-cons, quadratic constraints in Figure 12 are active in some intervals, which provides a slightly different closed-loop response.

Summing up, in normal operation all the control strategies evaluated perform similarly.

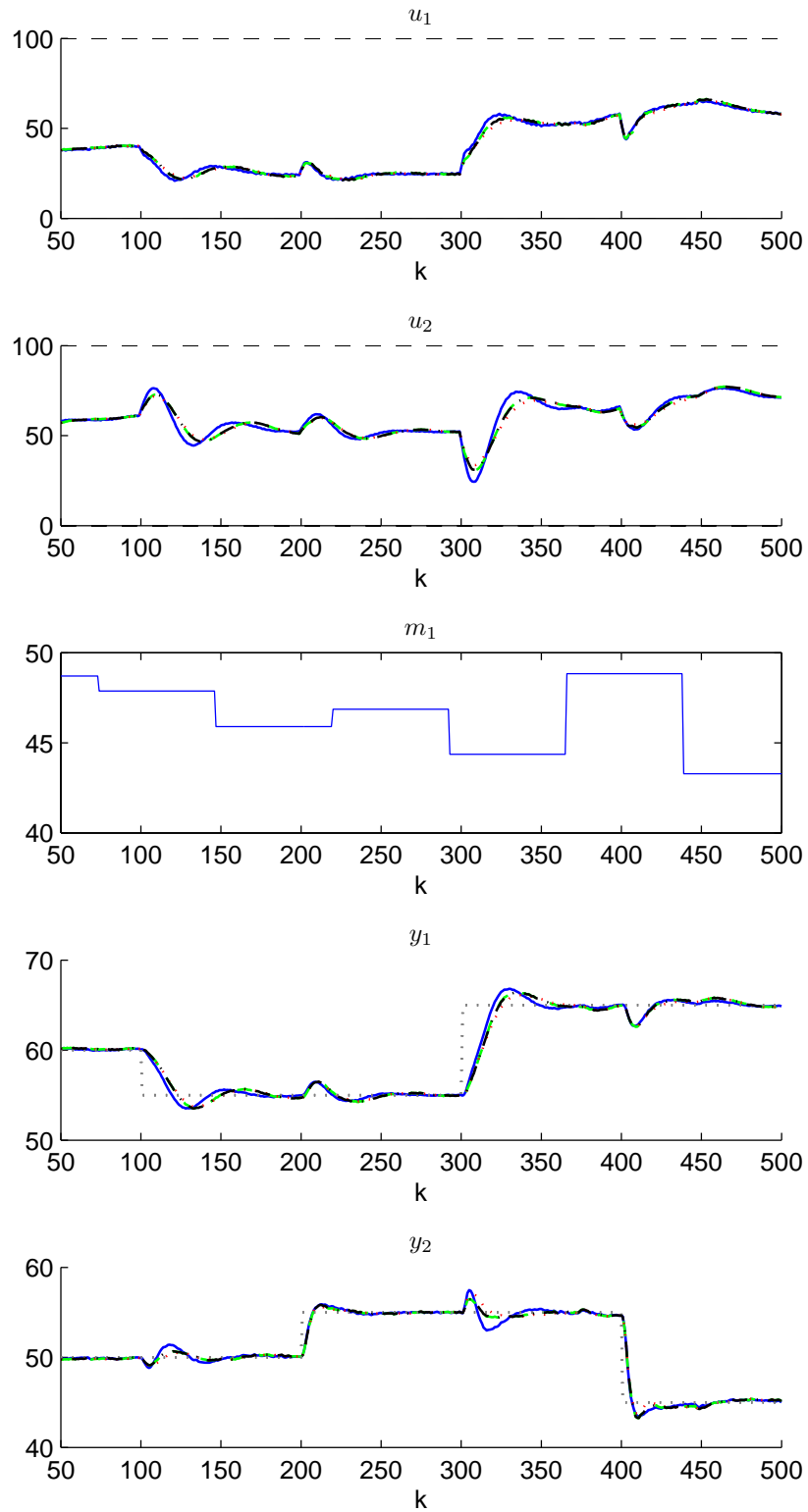


Figure 11: Closed-loop time response in normal operation. DM, continuous blue line; LV-MPC, dashed green line; LV-MPC-cons, dotted red line; LV-MPC-cons-neg, dash-dotted black line.

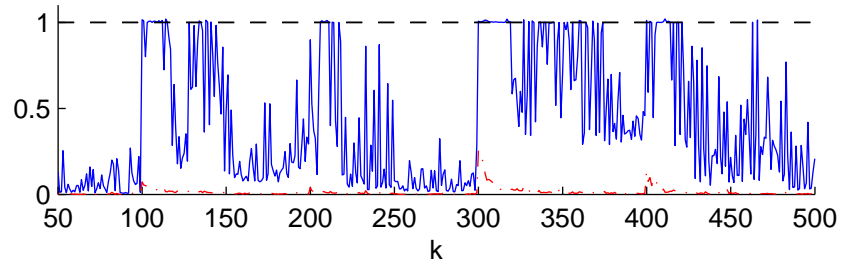


Figure 12: LV-MPC-cons: \bar{J}_t , continuous blue line; \bar{J}_e dash-dotted red line.

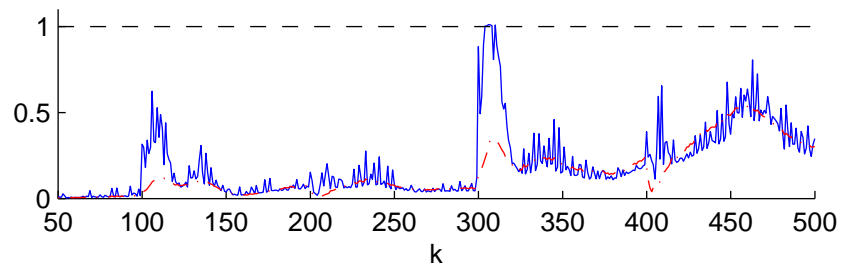


Figure 13: LV-MPC-cons-neg: \check{J}_t , continuous blue line; \check{J}_e dash-dotted red line.

5.5. Control results: large changes in set points and disturbance

The control strategies are evaluated in a situation different to that in the identification data set. Three events happen during the experiment: first a large change in the set point for y_1 , second a large change in the disturbance m_1 , and third a large change in the set point for y_2 . From the closed-loop response in Figure 14:

- DM: Presents the strongest interaction, but can reach any point as model validity is not ascertained.
- LV-MPC: Equivalent to DM, but has less d.o.f..
- LV-MPC-cons: Interaction to a change in y_1 is considerably reduced as the predictor is used in the range in which it is valid. From Figure 15, \bar{J}_t is at the boundaries of constraints continuously, and \bar{J}_e increases when m_1 changes. Constraints on \bar{J}_t and \bar{J}_e reduce interaction and provide better control if the process is in the area in which it has been identified. However, the resulting control is biased when there is a change in y_2 because the process is being operated considerably outside the identification region.
- LV-MPC-cons-neg: Interaction to a change in y_1 is considerably smaller to that obtained in DM and LV-MPC, but slightly above that obtained if past is not neglected. From Figure 16, \check{J}_t and \check{J}_e go to saturation only when changes happen in the experiment. Neglecting past data relaxes constraints on validity and prevents the controller from being biased.

Summing up, constraints on validity of the model neglecting past data can provide better results in the event of situations not included in the identification experiment.

Finally, the difference between linearising quadratic constraints at $\Delta \mathbf{t}_{d_{ti}}$ and at $\Delta \mathbf{t}_{d_i}$ is compared in Figure 17. The mean value of the constraint for the different instants of the control experiment versus the number of iteration of the sequential QP is represented. The continuous blue plot represents the value of \bar{J}_t linearising at $\Delta \mathbf{t}_{d_{ti}}$, and the dashed red plot represents the value of \bar{J}_t linearising at $\Delta \mathbf{t}_{d_i}$. In the first iteration the QP runs with no linearised constraint, and so both approaches present the same value of \bar{J}_t . For the second iteration, the approach linearising at $\Delta \mathbf{t}_{d_{ti}}$ provides a mean value of \bar{J}_t closer to 1. In both approaches \bar{J}_t converges to 1, but if the linearisation is performed at $\Delta \mathbf{t}_{d_{ti}}$, the algorithm converges at a faster rate. In real-time applications, computing time bounds the maximum number of iterations of the QP to implement, hence a faster convergence can be of importance. Therefore, linearising at $\Delta \mathbf{t}_{d_{ti}}$ is better than linearising at $\Delta \mathbf{t}_{d_i}$.

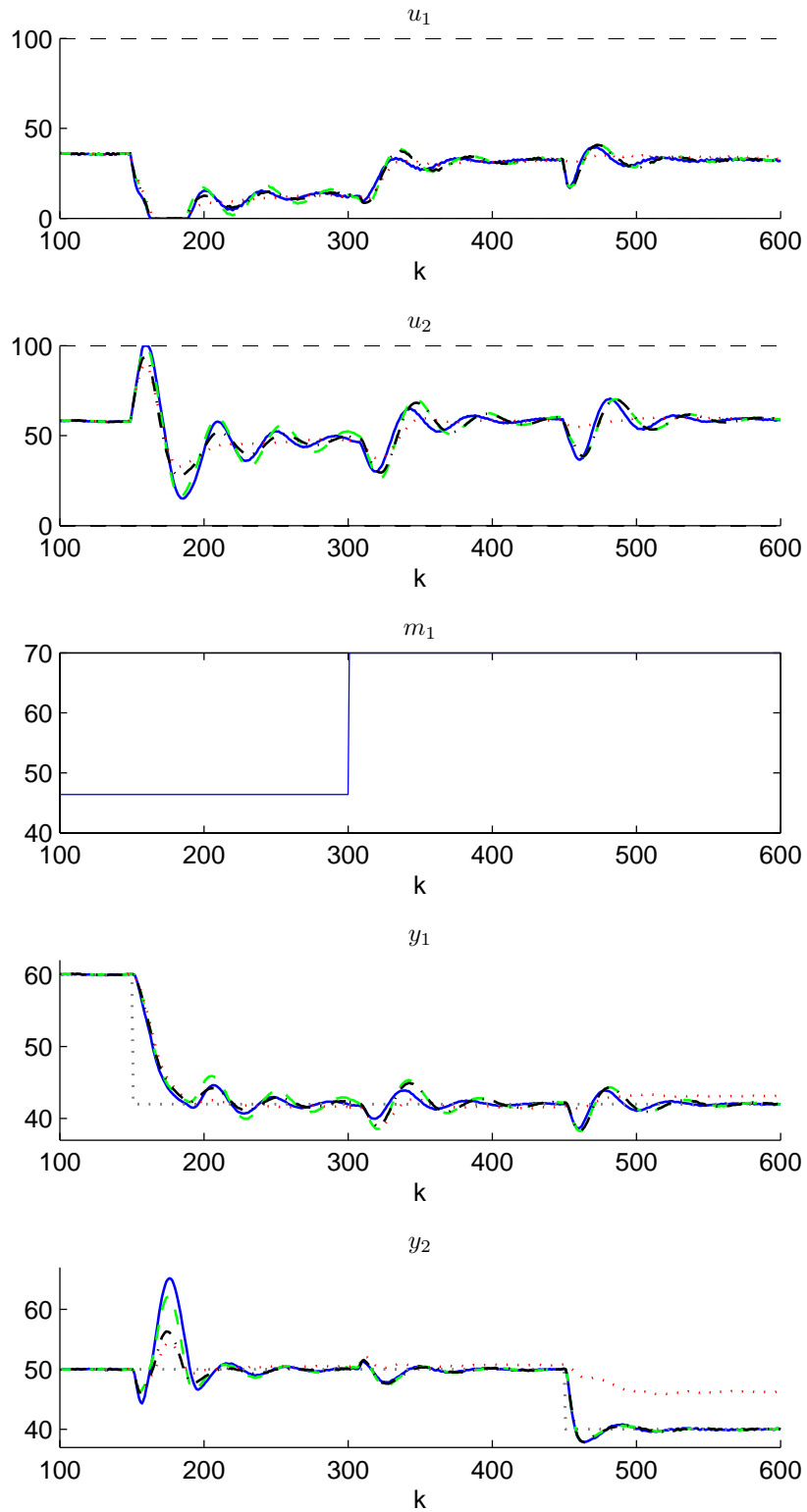


Figure 14: Closed-loop time response in the event of a large change in the set point for y_1 . DM, continuous blue line; LV-MPC, dashed green line; LV-MPC-cons, dotted red line; LV-MPC-cons-neg, dash-dotted black line.

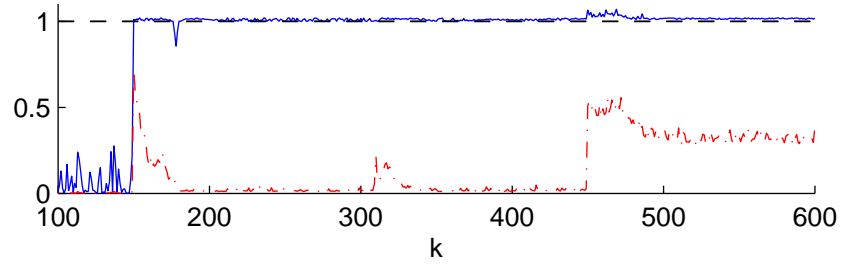


Figure 15: LV-MPC-cons: \bar{J}_t , continuous blue line; \bar{J}_e dash-dotted red line.

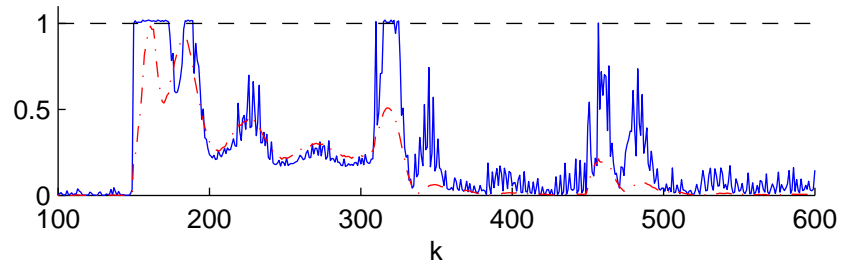


Figure 16: LV-MPC-cons-neg: \check{J}_t , continuous blue line; \check{J}_e dash-dotted red line.

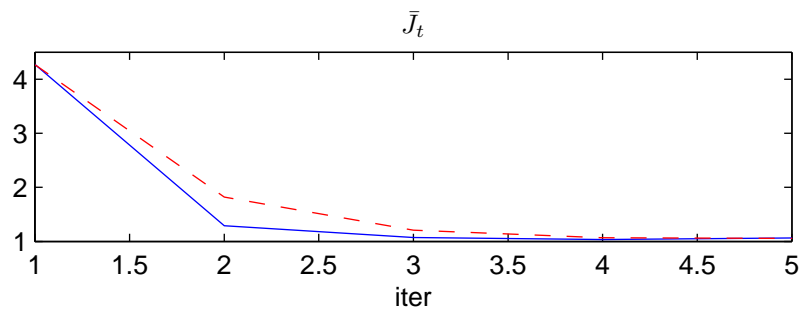


Figure 17: Decrease rate of \bar{J}_t . Linearising at $\Delta t_{d_{ti}}$, continuous blue line; linearising at Δt_{d_i} , dashed red line.

6. Conclusions

This paper proposes a strategy to ascertain validity of predictions in LV-MPC. Validity of predictions is important in that closed-loop performance of the controller heavily relies on the quality of predictions. Performing predictions outside the area in which the predictor has been identified implies extrapolation and can lead to poor predictions.

The proposed strategy for validity of predictions in LV-MPC defines two indicators based on Hotellings' T^2 and squared residuals of projection in the input space. The indicators proposed neglect past data, and it is shown through an example how considering the indicators that neglect past data can provide better results. The reason is adding constraints on validity indicators provides a conservative framework to regulate extrapolation and neglecting the past relaxes such conservative framework while ensuring validity of predictions in terms of decisions on the manipulated variables. The added constraints can lead to a biased control if the current situation is not contained in the identification data set and extrapolation is not allowed, especially if past data is considered in the validity indicators.

The proposed indicators are quadratic expressions in the variable of minimization, which yields a QCQP to be solved on-line at each sampling instant. The strategy adopted to solve the QCQP is a sequence of QPs. The advantage of such an approach is with one iteration there is one solution available, and such solution can be improved accounting for quadratic constraints as long as there is remaining computing time. Constraints are linearised not at the current point, but at the boundary of the constraint aligned with the current point and the minimum of the validity indicator. It is shown through an example how this approach reduces the value of the validity indicator at a faster rate.

Finally, it has been shown through an MIMO example that better closed-loop results can be obtained using the proposed strategy to ensure validity of predictions in LV-MPC. Some guidelines for future work include adding measurable disturbances to the model, and programming the controller to run in a real time target and use it to control fast real processes on-line.

Acknowledgments

The first author is recipient of a fellowship from the Spanish Ministry of Science and Innovation (FPU AP2007-04549). This paper is partially funded by projects DPI2008-02133/DPI, TIN2011-28082 and PROM-ETEO/2012/028. The authors gratefully acknowledge reviewers' comments.

References

- [1] H. A. L. Kiers, A. K. Smilde, A comparison of various methods for multivariate regression with highly collinear variables, *Statistical Methods and Applications* 16 (2007) 193–228.
- [2] E. F. Camacho, C. Bordons, *Model Predictive Control*, Springer, 2004.
- [3] S.-L. Jämsä-Jounela, Future trends in process automation, *Annual Reviews in Control* 31 (2007) 211–220.
- [4] P. Thwaites, Process control in metallurgical plants-from an Xstrata perspective, *Annual Reviews in Control* 31 (2007) 211–239.
- [5] J. Flores-Cerrillo, J. MacGregor, Latent variable MPC for trajectory tracking in batch processes, *Journal of Process Control* 15 (2005) 651–663.
- [6] D. Laurí, J. Rossiter, J. Sanchis, M. Martínez, Data-Driven Latent-Variable Model-Based Predictive Control for Continuous Processes, *Journal of Process Control* 20 (2010) 1207–1219.
- [7] J. A. Rossiter, B. Kouvaritakis, Modelling and implicit modelling for predictive control, *International Journal of Control* 74 (2001) 1085–1095.
- [8] R. Kadali, B. Huang, A. Rossiter, A data driven subspace approach to predictive controller design, *Control Engineering Practice* 11 (2003) 261–278.
- [9] R. Cagienard, P. Grieder, E. Kerrigan, M. Morari, Move blocking strategies in receding horizon control, *Journal of Process Control* 17 (2007) 563–570.
- [10] L. Wang, *Model Predictive Control System Design and Implementation Using Matlab*, Springer, 2009.
- [11] N. Blet, D. Megías, J. Serrano, C. de Prada, Non linear MPC versus MPC using on-line linearisation - a comparative study, in: *IFAC*, 2002.
- [12] S. J. Qin, T. A. Badgwell, A survey of industrial model predictive control technology, *Control Engineering Practice* 11 (2003) 733–764.
- [13] J. Flores-Cerrillo, J. MacGregor, Control of batch product quality by trajectory manipulation using latent variable models, *Journal of Process Control* 14 (2004) 539–553.
- [14] A. Höskuldsson, PLS regression methods, *Journal of Chemometrics* 2 (3) (1988) 211–228.
- [15] H. Martens, Reliable and relevant modelling of real world data: a personal account of the development of PLS Regression, *Chemometrics and Intelligent Laboratory Systems* 58 (2001) 85–95.
- [16] S. Boyd, L. Vandenberghe, *Convex Optimization*, Cambridge University Press, 2004.
- [17] B. Huang, R. Kadali, *Dynamic Modeling, Predictive Control and Performance Monitoring: A Data-driven Subspace Approach*, Springer, 2008.
- [18] G. Pellegrinetti, J. Bentsman, Nonlinear control oriented boiler modelling - a benchmark problem for controller design, *IEEE Transactions on Control Systems Technology* 4 (1996) 57–64.
- [19] Y. Zhu, F. Butoyi, Case studies on closed-loop identification for MPC, *Control Engineering Practice* 10 (2002) 403–417.
- [20] Y. Zhang, Enhanced statistical analysis of nonlinear processes using KPCA, KICA and SVM, *Chemical Engineering Science* 64 (2009) 801–811.

Biographies

D. Laurí was born in 1983 in Alicante, Spain. He received the B.Sc. degree in Control Automation Engineer in 2007 at the Polytechnic University of Valencia (UPV), honoured with academic efficiency awards. He received a training grant at ALCOA (ALuminium Company of America) as a process engineer for

a year. In 2008, he obtained master degree in Automatics and Industrial Informatics at UPV. Since then he has been a Ph.D student at the Department of Systems Engineering and Control at UPV. His research interests include model-based predictive control relevant identification, identification of MIMO processes in presence of co-linearity in the data set, and control in the space of latent variables.

J. Sanchis received his B.Sc.(1993) and Ph.D. (2002) in Computer Science from Universidad Politécnica de Valencia (Spain). He is a professor in the Department of Systems Engineering and Control of the same university. His main research interests are multivariable predictive control, process optimization and computational intelligence methods for control engineering.

M. Martínez is a professor in the Department of Systems Engineering and Control of the Polytechnic University of Valencia (Spain). He has a B.Sc. and a Ph.D. degree from the same university. He has three years of industrial experience in control engineering in cement plants. He has published more than 30 papers in journals of JCR (<http://personales.upv.es/~mmiranzo>), and numerous papers in conference proceedings, chapters of control books and a complete book by Prentice-Hall, this book is devoted to Identification and Adaptive Control. His research interests are applied adaptive control, predictive control, fuzzy logic, genetic algorithms and multiobjective optimization, etc. During the 90's he was associated at Department of Engineering Science of Oxford University (U.K.) during a short term working with professor D. W. Clarke and his colleagues in a promising new area, genetic predictive control.

A. Hilario is a lecturer and researcher in the Department of Systems Engineering and Control of the Polytechnic University of Valencia (Spain). He has a B.Sc. degree from the Spanish National University of Distance Education. He has three years of experience in control engineering in the water-supply Industry. His main research interests are identification and control of high-performance pneumatic actuators.



(a) D. Laurí



(b) J. Sanchis



(c) M. Martínez



(d) A. Hilario